INTERNATIONAL JOURNAL OF PRECISION ENGINEERING AND MANUFACTURING Vol. 16, No. 11, pp. 2339-2346 OCTOBER 2015 / 2339
DOI: 10.1007/s12541-015-0301-0 ISSN 2234-7593 (Print) / ISSN 2005-4602 (Online)

# Effects of Cavity Size and Density on Polymer Micro Hot Embossing

**Xiang Zhang[1,2,3], Ge Fang[1,2,3], Tengjiao Jiang[1], Na Zhao[2,3], Junfeng Li[1,2,3], Bowen Dun[1,2,3], and Qian Li[1,2,3,#]**

1 School of Mechanics & Engineering Science, Zhengzhou University, Zhengzhou, 450-001, China
2 National Center for International Joint Research of Micro-Nano Molding Technology, Zhengzhou University, Zhengzhou, 450-001, China
3 Key Laboratory for Micro Molding Technology of Henan Province, Zhengzhou University, Zhengzhou, 450-001, China
# Corresponding Author / E-mail: qianli@zzu.edu.cn, TEL: +86-371-6778-1750, FAX: +86-371-6778-1237

KEYWORDS: PMMA, Micro hot embossing, Picoseconds laser, Cavity density, Micro mold

*We designed nine micro molds with various cavity geometric parameters to investigate their effects on micropillars replication of the amorphous polymer via micro hot embossing. Picoseconds laser was used to fabricate the micro holes array on the stainless steel plates with 200 μm thickness as micro molds. The mechanical behavior of PMMA above glass transition temperature was investigated by uniaxial compression tests at various temperatures and strain rates, the results were used in simulation as constitutive relation. Confocal microscope and optical microscope showed that the replication height has a complicate nonlinear relationship with cavity size and density. DEFORM 3D was used to model and simulate the embossing process, and it is a good approach to investigate the micropallars replication heights, front angles and filling ratios.*

Manuscript received: April 20, 2015 / Revised: July 31, 2015 / Accepted: August 3, 2015

**NOMENCLATURE**

AR = aspect ratio of micro mold
CD = cavities density of micro mold
D = diameter of micro cavity
H = height of embossed micropillar
DC = distance between centers of nearest micro cavity
DE = distance between edges of nearest micro cavity
FEA = finite element analysis

## 1. Introduction

Micro hot embossing is one of the most popular fabrication methods to replicate polymer micro features in the field of micro-devices.[1,2] These micro features can be widely used in valve, turbine, needle, chemical mixers, micro medical tools and other productions of micro engineered system. Micro hot embossing should be formed in a single step process, otherwise multiple processing steps are needed by using the conventional lithographic processes on glass or semiconductor substrates.[3] Accordingly, this process can be the alternatives of the cost effective and high volume fabrication for microfluidic[4] and micro optical components such as wave-guides and lenses.[5] In recent years, many researches on micro hot embossing are reported and divided into several categories in general.

(1) Processing and optimization. Hot embossing process under various forming conditions such as forming temperature, load, and holding time in pressing were investigated. Lee et al.,[6] Singh et al.,[7] and Lin et al.[8] demonstrated that the depth of replicated patterns increased in proportion to increasing forming temperature, load and holding time which are main process conditions to be optimized.[9,10] The demolding is the last and critical stage of micro hot embossing, the force required to separate a polymer part from the mould should be minimized to avoid the generation of structural defects for the produced micro structures. Omar et al.[11] proposed an analytical model to predict the required demolding force in hot embossing.

(2) Modelling and simulation. Srivastava et al.[12] developed a thermo-mechanically-coupled large-deformation isotropic elastic-viscoplastic theory for amorphous polymers in a temperature range which spanned their glass transition temperature. Zhang et al.[13] drew the conclusion from FEA results that the small duty ratio cavity filled more sufficiently than the large duty ratio cavity. With the same cavity duty ratio, the inner cavity filled more quickly and sufficiently than the outer cavity. In the past, filling, cooling and demolding in a micro hot

embossing process are modeled independently. Jha et al.[3] presented a comprehensive integrated simulation of the hot embossing process. As the parameters in each of these stages affect the final quality of products, the simulations were performed using the software of DEFORM 3D with transferring the strain history from one stage to another. Thus, the final product quality is a function of the preceding quality in each stage. He et al.[14] designed an access slot and block as the flow barriers to enhance polymer filling. FEA results demonstrated that those designs could accelerate polymer filling speed and improve filling efficiency.

(3) Micro mold fabrication. Some of the present micro fabrication processes include LIGA, reaction ion etching, micro machining, powder injection molding (PIM) and micro laser ablation. In general, the mold is made of silicon, which is brittle and fails after producing a limited number of parts. Metallic molds produced by micro-machining have a much longer life; however, the surface finish of the mold is not good for fabricating polymeric devices which good surface finish is required. Recently, some researchers developed metallic glass micro mold fabricated by superplastic forming with a silicon master, which could produce high quality and high strength molds with long life span.[15,16] However, metallic glasses are rather costly, Tran et al. explored the manufacture of an aluminum alloy (AA6061-T6) mold by hot embossing using a silicon master.[17] With the development of micro machining technology, more and more materials can be used by various micro fabrication methods. In this work, the picosecond laser micromachining technology was applied to fabricate micro holes array in stainless steel substrate as micro mold.

The results also illustrated the effects of mold geometric structure on polymer filling. However, there is still dearth of systematic study on effects of mold structure on micro hot embossing. The purpose of this paper is to design and fabricate micro molds with various dimensions and to investigate two key parameters, the cavity diameter and density.

## 2. Experiments

### 2.1 Micro mold fabrication

Micro mold is a critical micro-replication tool for micro hot embossing. Laser micro-processing is an enabling technology that has developed rapidly over the last decade. It is being applied across many industries, including semiconductors, electronics, medical, automotive, aerospace, instrumentation and communications.[18,19] Using ultra-short pulsed (picosecond) lasers with material-adapted wavelengths the quality of the ablation process can be increased significantly compared to long pulses. In nanosecond laser processing this energy transfer occurs during the duration of the laser pulse, whereas in picosecond laser processing the energy transfer occurs after a certain interaction time. For metals, this transfer time is generally in the range of some picoseconds.

Picosecond laser micromachining was used to fabricate micro mold in this work. We designed nine micro molds with different cavity geometric parameters in order to study the effects of cavity size and density on polymer micro hot embossing. Stainless steel 304 was chosen as mold material which thickness is 200 $\mu$m. Table 1 shows the geometric dimensions of designed nine micro molds. Molds were divided into A, B and C three groups as shown in Table 1. Each group has includes three molds which have the same cavity size but different DC and DE.

Table 1 Geometric dimensions of micro molds

| Mold No. | D ($\mu$m) | DC ($\mu$m) | AR | CD |
|---|---|---|---|---|
| A1 | 300 | 600 | 0.67 | 0.196 |
| A2 | 300 | 500 | 0.67 | 0.283 |
| A3 | 300 | 400 | 0.67 | 0.442 |
| B1 | 200 | 500 | 1 | 0.126 |
| B2 | 200 | 400 | 1 | 0.196 |
| B3 | 200 | 300 | 1 | 0.349 |
| C1 | 100 | 400 | 2 | 0.049 |
| C2 | 100 | 300 | 2 | 0.087 |
| C3 | 100 | 200 | 2 | 0.196 |

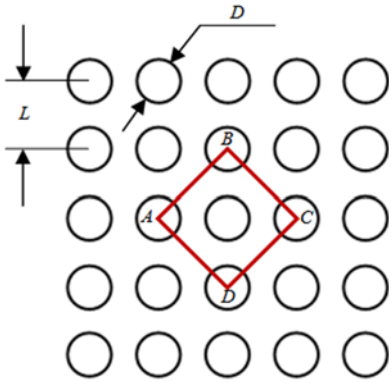


Fig. 1 The diagram of aspect ratio and cavities density

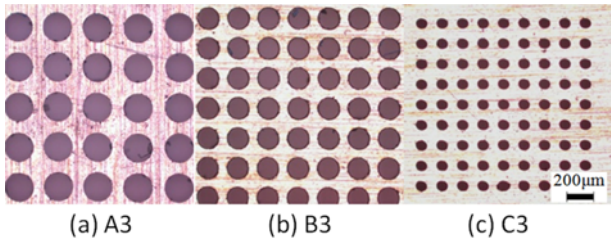


Fig. 2 The micro molds fabricated by picosecond laser processing

Fig. 1 shows the diagram of holes array in micro mold. Aspect ratio (AR) is defined as H/D, cavities density (CD) is defined as Sc/St. Four points A, B, C, D are the nearest holes center to one cavity. Here, Sc is the area of cavities in square ABCD, and St is the area of total square ABCD. In Fig. 1, Sc is equal to double area of holes exactly.

DeepPioneer (Deli Laser Solutions Co., Ltd., Jiangyin, China) was used to drill micro holes array in the plates which are presented in Fig. 2.

### 2.2 PMMA mechanical property above Tg

During the hot embossing process, polymer substrate is heated above glass transition temperature ($T_g$) and pressed by upper tool to deform. Study on the mechanical property of polymer is conducive to reveal its constitutive equation above $T_g$. The standard uniaxial compression tests were performed to PMMA at different strain rates and

Table 2 The parameters of uniaxial compression tests

| Temperature (°C) | Strain rate ($s^{-1}$) |
|---|---|
| 110 | 0.1 |
| 120 | 0.01 |
| 130 | 0.001 |

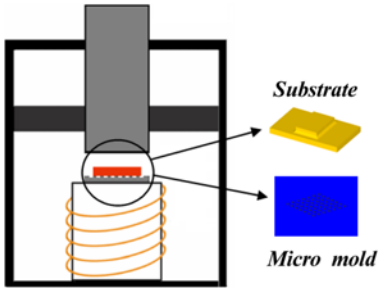


Fig. 3 Schematic diagram of the micro hot embossing

temperatures. Table 2 shows the parameters of uniaxial compression test in which three strain rates (0.1, 0.01 and 0.001$s^{-1}$) are applied at each temperature respectively. Flow stress-flow strain curves are acquired to further study by numerical simulation.

ASTM Standard D 695-02a recommends an aspect ratio of 2.0 for compression testing of rigid plastics. However, Dupaix and Castro[20] revealed that a wide deviation based on this standard is common through a literature search. Zaroulis and Boyce[21] found in testing polycarbonate samples with initial height to diameter ratio in the range of 0.4-1.1 that initial height to diameter ratio had no effect on the measured stress-strain behavior. Therefore, an initial height to diameter ratio of 0.6875 was chosen for the PMMA specimen with diameter 8mm and height 5.5mm, fabricated by injection molding. The $T_g$ of the PMMA used was determined by DSC (DSC2020, TA) and it was 100°C approximately.

The test specimens were placed between two compression platens with a light amount of WD-40 lubricant between the specimen and the platens in order to minimize friction. To ensure that the platens were at the appropriate testing temperature, the oven and platens were allowed to equilibrate for two hours before testing. The air temperature inside the chamber was monitored by a thermocouple. Once a specimen was ready, the measure time lasted for 30 minutes. This not only heated the polymer to the test temperature and achieved thermal equilibrium between the specimen and platens, but also relieved internal stresses induced during specimen fabrication.

Experiments were conducted using constant true logarithmic strain rate, and specimens were compressed to a final true strain of 1.0. Instron 5585 screw driven load frame with a 20 kN load cell and an Geger RGW-300 high temperature environmental chamber (Shenzhen Geger Instrument Co., Ltd.) were used.

### 2.3 Polymer micro hot embossing

PMMA (CP-51a, Lucite) was used in this study. The polymer sample plates were prepared by micro injection molding which size is 10mm×10mm×1mm.Generally, there are four different hot embossing modes.[22] We chose the direct open-die embossing mode in this work.

Table 3 The parameters of hot embossing experiments

| Process parameter | Value |
|---|---|
| $T_m$ (°C) | 130 |
| Pre-load (N) | 1 |
| Stroke speed (mm/s) | 0.01 |
| Pre-heating time (min) | 6 |
| Holding pressure time (s) | 0 |
| Total stroke (mm) | 0.4 |

Fig. 3 shows the schematic of the experimental set-up. Micro hot embossing process was carried out on an SUNS-UTM2203 (Shenzhen, China) universal materials testing machine to replicate micropillars with stainless steel micro mold to the polymer substrates. Heating temperature above $T_g$ to emboss the polymer substrate on micro mold with specific pressure or die speed. The load limit of the testing machine was 2 kN. The accuracy of loading was controlled to be within ±0.01 N.

PMMA substrates used in micro hot embossing were prepared by micro injection molding (Babyplast6/10P). The geometric structure of PMMA substrate is apt to demolding. In all embossing experiments for nine molds, the uniform process parameters were setting as Table 3. Heating stage was set at 130°C, The PMMA substrates was put on the stage and pressured by a preload as 1 N for 6 minutes to pre-heating due to the low thermal conductivity of polymer. Hot embossing was performed by at a constant rate, and stopped when the embossing pressure reach the applied load. The embossed substrate was put into water (room temperature) quickly to solid the polymer. The experiments were repeated at least five times for each micro mold. Leica CM1850 was used to cut the embossed polymer substrates to study the cross-section of micro pattern. Laser confocal microscope (LEXT OLS 4100) and optical microscope (Olympus BX 51) were also used to measure the replication heights.

### 2.4 Modeling and simulation of micro hot embossing

Material processing simulation is a good approach to investigate the micro patterns replication with hot embossing. In this work, commercial software DEFORM 3D was used to model and simulate the embossing process. This software is based on rigid-plastic finite element method that proposed by Lee and Kobayashi[23] early in 1970's. The geometry models of the molds and polymer substrate are generated in UG NX 8.5 and then are transferred in the STL file format to DEFORM 3D. The micro mold acts as a bottom die and PMMA as a workpiece since it undergoes deformation. The mold is placed on the work piece such that both the surfaces are in contact. In order to reduce the total mesh quantity, one quarter of workpiece was investigated in this work, and symmetric boundary was used in the FEM model.

Plastic flow data is fundamental to simulations because it governs deformation and flow behavior for any object undergoing permanent deformation. Flow stress required for deformation is generally given as a function of plastic strain, strain rate and temperature. DEFORM provides different methods of defining the flow stress. The tabular format is the most versatile format in that it can represent any material where flow stress can be given as a function of strain, strain rate, and temperature. Therefore, this format is selected in the study shown as following equation.

$$\overline{\sigma} = f(\bar{\varepsilon}, \dot{\bar{\varepsilon}}, T) \quad (1)$$

where $\overline{\sigma}$ is plastic flow stress, $\bar{\varepsilon}$ is effective plastic strain, $\dot{\bar{\varepsilon}}$ is effective plastic strain rate and $T$ is temperature. The flow stress-flow strain relationship for PMMA used in this work was determined by experiments, detail in section 3.1.

In general, most metal forming processes are not extremely sensitive to friction, and the typical values are perfectly adequate. However, the friction factor of PMMA and stainless steel 304 near the $T_g$ of PMMA isn't reported yet and difficult to obtain by experiment directly. A method is proposed in this work to determine the value through the validation of simulations and experiments, more details can be found in section 3.3.

## 3. Results and Dicussion

### 3.1 The constitutive relation of PMMA above Tg

In general, the molecular chains of amorphous polymer begin to move when the temperature is beyond $T_g$. The polymer is assumed as a viscous fluid with lower viscosity. In order to obtain the constitutive relation, the relationship of temperature and strain rate with the mechanical behavior of amorphous polymer (PMMA) was investigated using uniaxial compression tests at various temperatures above the $T_g$ of PMMA.

Fig. 4 shows the strong strain rate dependence of PMMA for constant temperature of 110°C, 120°C and 130°C. The true stress - true strain curves in these figures show an initial elastic behavior, followed by a yield or flow event, with subsequent strain hardening, which increases at large strains. It shows that the initial modulus decreases dramatically at higher temperatures (such as 130°C), while at lower temperatures is relatively constant. The strain hardening is gentle in slope as the strain rate decreases from $0.1s^{-1}$ to $0.001s^{-1}$. Fig. 4(a) shows the flow stress decreases form 42MPa to 20MPa as the strain rate decreases from 0.1 $s^{-1}$ to 0.001 $s^{-1}$ when the true strains all reaches 0.9. The flow stress is even only about 1MPa when temperature is 130°C and strain rate is 0.001 $s^{-1}$.

Experimental results also show PMMA is sensitive to the temperature and the yield stress decreases with temperature increasing. The yield peak disappears behaving a good plasticity when the temperature is higher than 120°C. It is found that both increasing temperature and decreasing strain rate can decrease flow stress to reach same strain value. The C3 in Fig. 4(a) and C1 in Fig. 4(b) coincide with each other, and C2 curve in Fig. 4(b) and C1 curve in Fig. 4(c) also coincide with each other.

According to time-temperature equivalence principle of polymer, the same effect can be produced on the compliances or moduli either by a change of temperature or time-scale.[24] It means the same deformation of polymer will be performed by higher temperature or lower strain rate. Higher temperature means more energy consumption and more cooling time, lower strain rate means long process time and inefficiency for commercial production of micro hot embossing. Therefore, the suitable process condition should be chosen in accord with demand. In this work, the process condition was set as following,

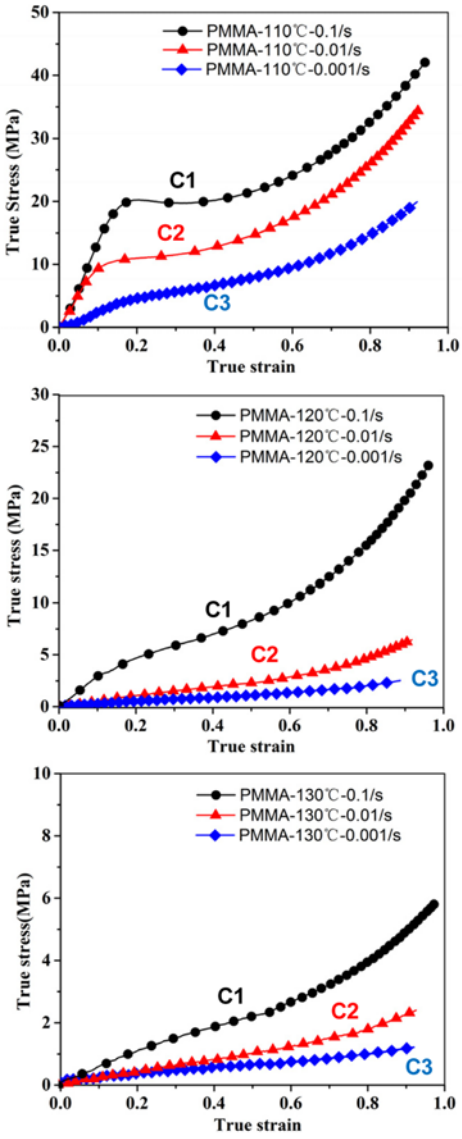


Fig. 4 Flow stress-strain curves of PMMA

embossing temperature is 130°C and top die stroke speed is 0.01 mm/s.

### 3.2 The replication of hot embossing

The micro hot embossing process for PMMA relies on many factors such as processing parameters, substrate thickness, molecule weight, pattern shape and size,[6] and even polymer orientation.[25] However, in this work, our study focused on the effects of two important geometric parameters of micro mold, cavities size and cavities density on pattern replication.

Fig. 5(a) shows the surface profile of micropillar array embossed by C3 mold. Shadow effect appeared around the roots of micropillars along the polymer flow direction. The shadow effect in the center (also is the pressure center of embossing) is not obvious than that of far away. Numerical simulation results also can explain the shadow effect. The effective strain pattern near micro cavities is presented in Fig. 5(b). There is no doubt that the shadow appeared areas are in accord with the high effective strain areas. As a consequence, the polymer large deformation happened in high strain area, however, not enough

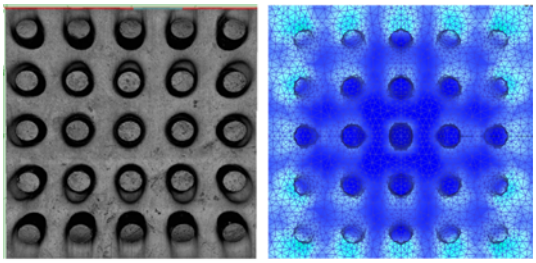


Fig. 5 Micropillar features embossed by A1 mold

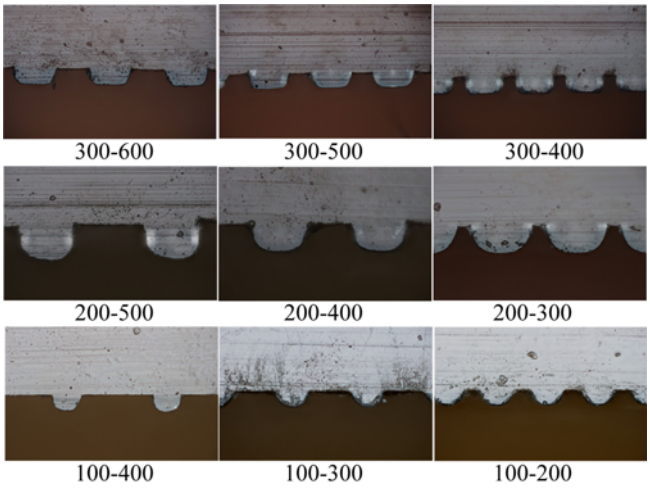


Fig. 6 Cutting profiles of micropillars embossed by various molds

polymer complemented from outside so that the sunken area appeared which looks like shadow.

Simultaneously, slope effect appeared in the top of most of cylinder are shown in Fig. 6. The double "S" effects (shadow effect and slope effect) are both raised by polymer flow from the center to edge during embossing process. Those effects should be weakened even disappeared if the temperature is higher and or enough holding pressure by means of appropriate mold structure.

### 3.2.1 Effect of cavity size on micro hot embossing

The experimental condition was restricted to be performed for nine molds. Fig. 6 shows the cutting profile of micropillars embossed by each mold. It was noteworthy that when the diameter of micro cavity is 300 $\mu$m, the cutting profile fronts of micropillars are flat, however, when the diameter of micro cavity is 200 $\mu$m or 100 $\mu$m, the cutting profile front of micropillars are curve. It can be anticipated that the diameter of micro cavity determine the flow mode of polymer front in micro cavities. It was also found that the replication heights decrease rapidly when the diameter is 100 $\mu$m compared with 200 $\mu$m and 300 $\mu$m.

In the diameter size range this work involved, the diameter is bigger, the replication height is higher. It means that the smaller the diameter of micro cavity, the more difficult polymer filling process and bigger embossing force is needed. Near closed die embossing should be used to improve polymer filling when the cavity diameter is below 200 $\mu$m.

According to the Hagen-Poiseuille law, the pressure difference between the ends of the circular cavity is proportional to the viscosity of polymer and the second power of cavity depth.

$$P = \frac{32\eta L^2}{td^2} \tag{2}$$

Here $P$ is the required pressure, $L$ is the depth of micro circular cavity, $\eta$ is the dynamic viscosity, $t$ is the filling time and $d$ is diameter of circular cavity. In this study, the top die speed is slow and the strain rate of polymer is not so high that the viscosity is considered as a constant. When $\eta$, $P$ are constants at any time, the height of embossed micropillar is linearly improved with an increase of cavity diameter as shown in Eq. (3).

$$L = \sqrt{\frac{Pt}{32\eta}}d \tag{3}$$

The experiment result value is about 60 $\mu$m when $D$ is 100 $\mu$m, and the values should be 120 $\mu$m and 180 $\mu$m respectively according to Eq. (3) when $D$ is 200 $\mu$m or 300 $\mu$m. It is found that the experiment results of 100 $\mu$m and 200 $\mu$m well in accordance with the Eq. (3). However, a deviation exists when D is 300 $\mu$m, this may be related to the polymer flow mode which determined by cavity size. The front profile is flat when $D$ is 300 $\mu$m, that of 100 $\mu$m and 200 $\mu$m are curves. The height of micropillar is measured from climax of profile to bottom surface.

$$L = \int_0^{t_1} \sqrt{\frac{P(t)t}{32\eta(t)}}Ddt \tag{4}$$

In fact, the $P$ and $\eta$ are not constant in hot embossing with fixed top die stroke speed, they are the function of time. The strict expression should be as Eq. (4).

The different flow mode related to cavity size can also be explained by plastic deformation theory. When cavity size is large enough (e.g., 300 $\mu$m), the plastic deformation zone is relatively small than the cavity area. Therefore, plastic deformation zone almost not affect the filling front profile which keep flat. However, the microscale effect appears when the cavity size is below 200 $\mu$m due to the cavity area is too small to be influenced by the plastic deformation zone around the edge of micro cavity.

### 3.2.2 Effect of cavities density on micro hot embossing

Cavities density is also an important geometric parameter of micro mold. Fig. 7 also shows the relationship between the replication height of polymer micropillar and the CD of micro mold. Compared with cavity size, the effect of CD on replication height is complicated. The curves present linear that the replication heights increase with an increase of cavities densities when the diameter is 300 $\mu$m. On the contrary, the replication heights decrease with an increase of cavities densities when the diameter is 100ìm. However, it is interesting to note that the replication heights decrease firstly, and then almost keep constant with an increase of cavities density when the diameter is 200 $\mu$m.

In general, there is little effect on replication height when the CD reaches a certain value if the cavity size is fixed. Different CD will affect the stress distribution near the inlet of every micro cavity which leads to the little different replication height in same cavity size.

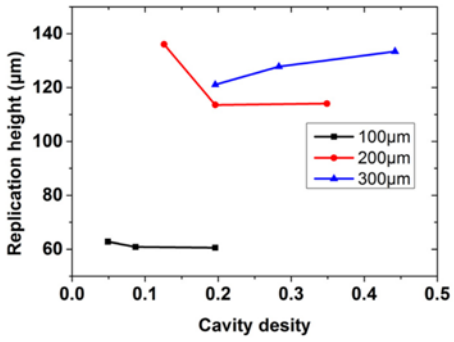


Fig. 7 The heights of micropillars embossed by various molds

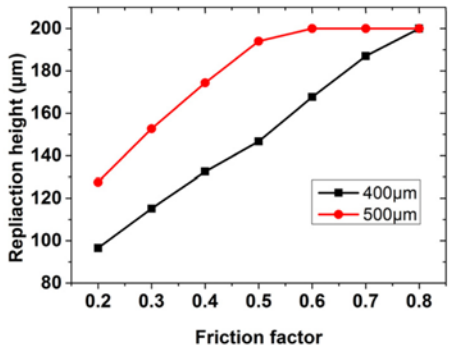


Fig. 8 The height of single micropillars by simulations with different friction factor

Table 4 The heights of micropillars embossed by the single hole mold

| Die stroke ($\mu$m) | Experimental results ($\mu$m) | | | | Simulation ($\mu$m) |
|---|---|---|---|---|---|
| | 1 | 2 | 3 | Average | |
| 400 | 123.6 | 129.5 | 126.7 | 126.6 | 125.4 |
| 500 | 158.3 | 163.2 | 161.1 | 160.9 | 163.6 |

### 3.3 The determination of friction factor in simulation

A series of simulations are performed by a mold with single hole ($D$ = 300 $\mu$m) under a uniform process setting only except the friction factor, which is set equal to 0.3, 0.4, 0.5, 0.6 and 0.7 respectively.

The results are shown in Fig. 8, the replication height is increasing with an increase of friction factor from 0.3 to 0.7 when the stroke of top die is 400 $\mu$m and 500 $\mu$m. Simultaneously, the corresponding embossing experiments were repeated three times. The real replication height was calculated by averaging three embossing experimental values as shown in Table 4. It was indicated that the effective friction factor ($f_{effective}$) should be in the range of 0.3 to 0.4 according to experimental results. Then, the $f_{effective}$ is obtained through linear interpolation by experimental values. Two friction factors are determined from two curves, and the average is 0.352.

As a result, we used this value as $f_{effective}$ to perform simulation again, and the results also are shown in Table 3. The deviation is below 2%. Therefore, the effective friction factor between PMMA substrates and the molds was determined as 0.352 and used in the following simulations.

Same series of simulations were performed to compare with the experiments as shown in Table 5. Most of the deviations are below 15%. The results revealed that the proposed method in the work is available to determine the effective friction factor. Simulations can take the place of many experiments to optimize original design and process.

Table 5 Average values and standard deviations of replication heights compared with simulation results

| Mold | DE | Experimental results ($\mu$m) | Simulation results ($\mu$m) |
|---|---|---|---|
| A1 | 300 | 121.14.9 | 156.8 |
| A2 | 200 | 127.88.2 | 161.7 |
| A3 | 100 | 133.44.4 | 152.6 |
| B1 | 300 | 136.04.7 | 121.7 |
| B2 | 200 | 113.68.9 | 111.2 |
| B3 | 100 | 114.14.8 | 113.9 |
| C1 | 300 | 62.81.8 | 69.8 |
| C2 | 200 | 60.92.0 | 66.9 |
| C3 | 100 | 60.60.8 | 68.3 |

Table 6 The front angle and filling area of micro cavity

| Mold | Experimental | | | Simulation | |
|---|---|---|---|---|---|
| | Angle (°) | Fill area ($cm^2$) | Fill ratio (%) | Angle (°) | Fill ratio (%) |
| A1 | 150.62.9 | 385.212.2 | 62 | 127.8 | 68 |
| A2 | 148.21.8 | 355.49.6 | 58 | 133.2 | 69 |
| A3 | 151.42.8 | 374.619.4 | 61 | 127.7 | 65 |
| B1 | 130.31.1 | 262.722.1 | 66 | 121.5 | 54 |
| B2 | 136.23.6 | 226.015.8 | 57 | 124.6 | 49 |
| B3 | 130.00.5 | 209.610.9 | 52 | 126.1 | 49 |
| C1 | 98.43.0 | 62.62.4 | 27 | 106.1 | 31 |
| C2 | 101.01.3 | 60.32.5 | 26 | 100.2 | 28 |
| C3 | 99.71.0 | 54.83.4 | 24 | 96.5 | 28 |

It was found that there are some deviations between simulation and experimental results in Table 5. The friction factor used in simulation was determined by single cavity mold. Thus, the edge of cavity effect on polymer filling was small. In case of the simulations of multi-cavities were performed, it can't be ignore. As a consequence, simulation results are higher than experimental results with the increase of cavity diameter.

The height of micropillar is an important value to evaluate the replication of hot embossing. However, the polymer front is not an absolute flat surface especially when the cavity diameter is below 200 $\mu$m and the measured height of micropillar is the maximum height of the front. The angle of front, filling area and filling ratio were also calculated and shown in Table 6.

As indicated in the table, the trend of the front angles and filling ratio is analogous to the replication height. Both values decreased with decreasing the cavity diameters. Compared with 200 $\mu$m and 300 $\mu$m, the front angle and filling ratio decrease rapidly when the cavity diameter is 100 $\mu$m. The influences of cavity density on the front angle and filling ratio are coincident with that on replication heights and can be ignored.

Fig. 9 shows the replication of micropillars embossed by high CD mold is more even than low CD mold. The slope effect is not so obvious with the increase of CD.

Same results are also found in Fig. 10, with increasing of CD, the heights of micropillars are more even, and the slope effect is not so obvious. The Z-axis normal stress decreases with the increase of CD because the polymer flow length is shortened and the lower pressure is

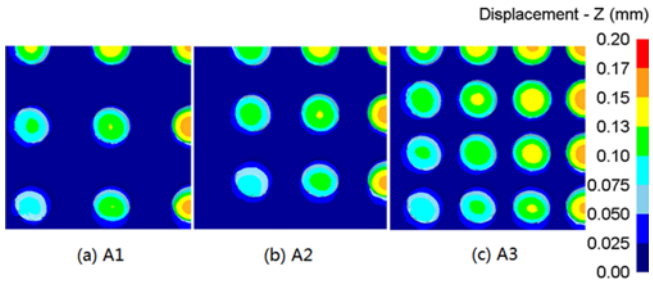


Fig. 9 The replication height of micropillars by simulation

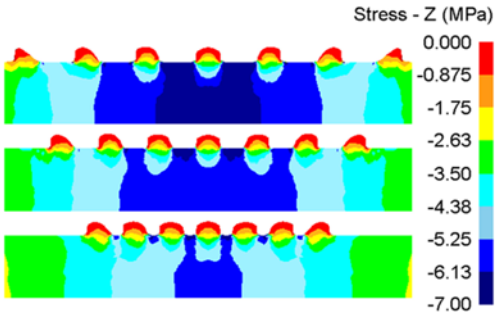


Fig. 10 The Z-axis stress profiles of PMMA substrates by mold Al, A2 and A3 when die stroke is 400 $\mu$m

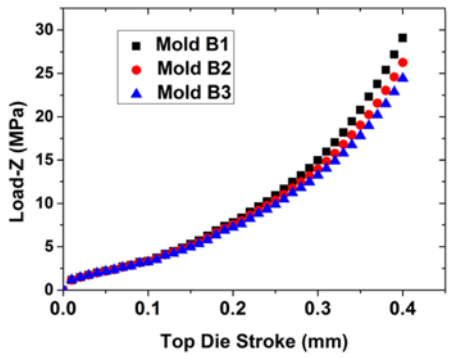


Fig. 11 The Z-axis load prediction with stroke increase

needed.

Similar results are also found in Group B ($D$ = 200 $\mu$m) and Group C ($D$ = 100 $\mu$m). Fig. 11 shows that the Z-axis loads increase with the top die stroke increase. When the stroke reaches 0.4 mm, the Z load of B1 is the biggest and B3 is the smallest. Because of the higher CD shortens the polymer flow length and lower Z-axis load is needed.

## 4. Conclusions

Various cavity geometric parameters of nine micro molds were prepared to investigate the cavity size and density effect on the micropillars replication of PMMA via micro hot embossing. The mechanical behavior of PMMA above $T_g$ showed that PMMA is sensitive to the temperature and the yield stress decreases with temperature increasing. The replication height of micropillars decreases with the micro cavity size (or diameter) decreased from 300 $\mu$m to 100 $\mu$m. Especially, when the diameter is down to 100 $\mu$m, the replication need more die stroke and the demolding is also more difficult. Little different replication height, front angle and filling ratio were affected by different cavity density in same cavity size. FEM model was build and the friction factor of PMMA near the $T_g$ is 0.352 used in simulation. Simulation results showed higher values than experimental results with the increase of cavity diameter and the replication of micropillars high CD mold is more even than that of low CD mold.

## ACKNOWLEDGEMENT

This work was financially supported by the National Natural Science Foundation of China (No.11372286), the Basic & Cutting-edge Technology Research Projects of Henan Province (No.132300410102), the Key Project of Science & Technology of Education Department of Henan Province (No.12A430018, 14A130001), and the Key Projects of Zhengzhou Science and Technology Bureau (No.121PPTGG360-4) are gratefully acknowledged.

## REFERENCES

1. Peng, L., Deng, Y., Yi, P., and Lai, X., "Micro Hot Embossing of Thermoplastic Polymers: A Review," Journal of Micromechanics and Microengineering, Vol. 24, No. 1, Paper No. 013001, 2014.
2. Gomez, J. A., Conner, G. T., Kim, Y.-J., Song, I.-H., and You, B. H., "Mold Filling Analysis of an Alignment Structure in Micro Hot Embossing," Fibers and Polymers, Vol. 15, No. 6, pp. 1197-1201, 2014.
3. Jha, J. S. and Joshi, S. S., "Numerical Simulation of Micro Hot Embossing of Polymer Substrate," Int. J. Precis. Eng. Manuf., Vol. 13, No. 12, pp. 2215-2224, 2012.
4. Sahli, M., Millot, C., Gelin, J.-C., and Barrière, T., "The Manufacturing and Replication of Microfluidic Mould Inserts by the Hot Embossing Process," Journal of Materials Processing Technology, Vol. 213, No. 6, pp. 913-925, 2013.
5. Heckele, M. and Schomburg, W., "Review on Micro Molding of Thermoplastic Polymers," Journal of Micromechanics and Microengineering, Vol. 14, No. 3, pp. R1-R14, 2004.
6. Lee, C.-S., Kang, C.-G., and Youn, S.-W., "Effect of Forming Conditions on Linear Patterning of Polymer Materials by Hot Embossing Process," Int. J. Precis. Eng. Manuf., Vol. 11, No. 1, pp. 119-127, 2010.
7. Singh, K. and Dupaix, R. B., "Hot-Embossing Experiments of Polymethyl Methacrylate across the Glass Transition Temperature with Variation in Temperature and Hold Times," Polymer Engineering & Science, Vol. 52, No. 6, pp. 1284-1292, 2012.

8. Lin, M.-C., Yeh, J.-P., Chen, S.-C., Chien, R.-D., and Hsu, C.-L., "Study on the Replication Accuracy of Polymer Hot Embossed Microchannels," International Communications in Heat and Mass Transfer, Vol. 42, pp. 55-61, 2013.

9. He, Y., Fu, J.-Z., and Chen, Z.-C., "Research on Optimization of the Hot Embossing Process," Journal of Micromechanics and Microengineering, Vol. 17, No. 12, pp. 2420-2425, 2007.

10. Liu, J., Jin, X., Sun, T., Xu, Z., Liu, C., et al., "Hot Embossing of Polymer Nanochannels using PMMA Moulds," Microsystem Technologies, Vol. 19, No. 4, pp. 629-634, 2013.

11. Omar, F., Brousseau, E., Elkaseer, A., Kolew, A., Prokopovich, P., and Dimov, S., "Development and Experimental Validation of an Analytical Model to Predict the Demoulding Force in Hot Embossing," Journal of Micromechanics and Microengineering, Vol. 24, No. 5, Paper No. 055007, 2014.

12. Srivastava, V., Chester, S. A., Ames, N. M., and Anand, L., "A Thermo-Mechanically-Coupled Large-Deformation Theory for Amorphous Polymers in a Temperature Range which Spans their Glass Transition," International Journal of Plasticity, Vol. 26, No. 8, pp. 1138-1182, 2010.

13. Zhang, T., He, Y., and Fu, J.Z., "Finite Element Modeling of Polymer Flow during Hot Embossing with Different Mold Structures and Embossing Conditions," Advanced Materials Research, Vol. 305, pp. 144-148, 2011.

14. He, Y., Fu, J., Zhao, P., and Chen, Z. C., "Enhanced Polymer Filling and Uniform Shrinkage of Polymer and Mold in a Hot Embossing Process," Polymer Engineering & Science, Vol. 53, No. 6, pp. 1314-1320, 2013.

15. Ma, J., Zhang, X., and Wang, W. H., "Metallic Glass Mold Insert for Hot Embossing of Polymers," Journal of Applied Physics, Vol. 112, No. 2, Paper No. 024506, 2012.

16. Zhang, X., Ma, J., Fang, G., Sun, B., Li, J., and Li, Q., "Polymer Micro Molding with Bulk Metallic Glass Mold," Microsystem Technologies, Vol. 21, No. 7, pp. 1453-1457, 2015.

17. Tran, N. K., Lam, Y. C., Yue, C. Y., and Tan, M. J., "Manufacturing of an Aluminum Alloy Mold for Micro-Hot Embossing of Polymeric Micro-Devices," Journal of Micromechanics and Microengineering, Vol. 20, No. 5, Paper No. 055020, 2010.

18. Jiang, T., Koch, J., Unger, C., Fadeeva, E., Koroleva, A., et al., "Ultrashort Picosecond Laser Processing of Micro-Molds for Fabricating Plastic Parts with Superhydrophobic Surfaces," Applied Physics A, Vol. 108, No. 4, pp. 863-869, 2012.

19. Knowles, M. R. H., Rutterford, G., Karnakis, D., and Ferguson, A., "Micro-Machining of Metals, Ceramics and Polymers using Nanosecond Lasers," The International Journal of Advanced Manufacturing Technology, Vol. 33, No. 1-2, pp. 95-102, 2007.

20. Palm, G., Dupaix, R., and Castro, J., "Large Strain Mechanical Behavior of Poly (Methyl Methacrylate)(PMMA) near the Glass Transition Temperature," Journal of Engineering Materials and Technology, Vol. 128, No. 4, pp. 559-563, 2006.

21. Zaroulis, J. S. and Boyce, M. C., "Temperature, Strain Rate, and Strain State Dependence of the Evolution in Mechanical Behaviour and Structure of Poly (Ethylene Terephthalate) with Finite Strain Deformation," Polymer, Vol. 38, No. 6, pp. 1303-1315, 1997.

22. KuduvaRamanThanumoorthy, R., and Yao, D., "Hot Embossing of Discrete Microparts," Polymer Engineering & Science, Vol. 49, No. 10, pp. 1894-1901, 2009.

23. Lee, C. H. and Kobayashi, S., "New Solutions to Rigid-Plastic Deformation Problems using a Matrix Method," Journal of Manufacturing Science and Engineering, Vol. 95, No. 3, pp. 865-873, 1973.

24. Bower, D. I., "An Introduction to Polymer Physics," Cambridge University Press, p. 204, 2002.

25. Jena, R. K., Taylor, H. K., Lam, Y. C., Boning, D. S., and Yue, C. Y., "Effect of Polymer Orientation on Pattern Replication in a Micro-Hot Embossing Process: Experiments and Numerical Simulation," Journal of Micromechanics and Microengineering, Vol. 21, No. 6, Paper No. 065007, 2011.